On the non-Gaussian nature of ionospheric vorticity

G. Chisham and M. P. Freeman

British Antarctic Survey, Cambridge, UK

G. Chisham, M. P. Freeman, British Antarctic Survey, Madingley Road, Cambridge, CB3 0ET, UK. (gchi@bas.ac.uk)

We present, for the first time, the probability density function (PDF) of ionospheric vorticity measurements made by the SuperDARN HF radars. We show that the PDF is typically heavy-tailed and best modelled by the q-exponential distribution across most of the ionosphere, except in the dayside region 1 current region where the Weibull distribution provides the best model. We identify these distributions as stationary solutions of a Fokker-Planck equation whose corresponding Langevin equation can be derived from the classic baroclinic and barotropic vorticity equations, respectively.

1. Introduction

As its alternative name suggests, the Gaussian probability distribution is commonly assumed to be the "normal" distribution for most types of fluctuations, due to it being the attractor distribution for sums of many independent random variables. However, in many cases in the human and natural world, it is leptokurtic (fatter than Gaussian) and heavy-tailed (fatter than exponential) probability distributions that are ubiquitous. The importance of these distributions lies in the high likelihood of large 'wild' fluctuations relative to a Gaussian distribution with the same variance. Or, equivalently, more of the variance is due to rare large deviations rather than frequent smaller deviations. Not having a full understanding of the distribution of fluctuations of a particular quantity, and just assuming that those fluctuations are normally distributed, can lead to highly flawed conclusions, such as an inadequate assessment of risk in financial models with disastrous consequences [*Mandelbrot and Hudson*, 2004]. Similar issues arise in the natural sciences where sometimes only the average values of certain quantities are known or used and the distributions of fluctuations are not considered, or assumed normal, leading to flawed results or conclusions [e.g., *Golovchanskaya*, 2008]. Furthermore, knowledge of the probability distribution of fluctuations can provide insight into the underlying dynamical processes, expressed by the Langevin equation corresponding to the Fokker-Planck solution [e.g., *Hnat et al.*, 2005].

In this paper, we compile the probability density function (PDF) of ionospheric vorticity measurements and investigate how the form of the PDF varies with spatial location within the polar ionosphere. We also fit a series of model distributions to the PDFs using

maximum likelihood estimates (MLEs) analysis and attempt to identify the best model that describes the observed distribution of vorticity. We interpret the model and its spatial variation in terms of the underlying magnetohydrodynamic processes. We conclude by proposing that a similar approach should be used for future studies of magnetic field-aligned current (FAC) fluctuations.

2. Method

The Super Dual Auroral Radar Network (SuperDARN) [*Greenwald et al.*, 1995; *Chisham et al.*, 2007] is a network of coherent scatter radars designed to measure large and meso-scale plasma flow in the Northern and Southern polar ionospheres. For this study we have used measurements from the Prince George/Kodiak SuperDARN radar pair in North America, during the years 2000 to 2005 inclusive. Measurements of magnetic field-aligned vorticity within the overlapping field of view of the two radars are determined according to Stokes' theorem by measuring the ionospheric plasma velocity around closed loops defined by the geometry of the overlapping radar beams [*Chisham et al.*, 2009]. Various loops may be constructed on differing scales. Here we use those on the smallest measurement scale which corresponds to closed loop areas ranging from $\sim$ 5000 km^2 closest to the radars to $\sim$ 50000 km^2 at the farthest overlapping ranges. Our analysis resulted in $\sim$6.2 million independent vorticity measurements during the 6-year interval over a wide range of altitude-adjusted corrected geomagnetic (AACGM) latitudes ($\sim$66°-85°) and the complete 24 hours of magnetic local time (MLT). In this paper, a positive (negative) field-aligned vorticity represents a clockwise (counter-clockwise) rotation when looking down the magnetic field into the Northern Hemisphere ionosphere.

We compare the probability distribution of measured vorticity ω at different locations with three candidate heavy-tailed model distributions:

(1) The exponential probability density function (PDF)

$$f_1(\omega) = \lambda e^{-\lambda\omega} \tag{1}$$

(2) The Weibull PDF (corresponding to a stretched exponential cumulative density function)

$$f_2(\omega) = \frac{c}{\chi}\left(\frac{\omega}{\chi}\right)^{c-1} \exp\left[-\left(\frac{\omega}{\chi}\right)^{c}\right] \tag{2}$$

where the function tends to an exponential as c tends to 1.

(3) The q-exponential PDF

$$f_3(\omega) = \frac{1}{\kappa}\left(1 - \frac{(1-q)\omega}{\kappa}\right)^{q/(1-q)} \tag{3}$$

where the function tends to an exponential as q tends to 1. (This is the form as given in *Shalizi et al.*[2007] - the function is also written in an alternative form with $q' = 1/(2-q)$).

The parameters of each model distribution are estimated using maximum likelihood (ML). Specifically the maximum likelihood estimates (MLEs) have been determined from an analytical or numerical solution of the stationary points of the log likelihood function [*Edwards et al.*, 2007; *Qiao and Tsokos*, 1994; *Sornette*, 2003; *Shalizi et al.*, 2007]. In this process, we consider the negative and positive vorticities as separate distributions because the PDFs for the different polarities appear distinctly different. Hence, we have two vorticity data sets, $\boldsymbol{\omega}_+ = \{\omega_1, \omega_2, \omega_3, ..., \omega_{n_+}\}$ for $\omega_i > 0$, and $\boldsymbol{\omega}_- = \{|\omega_1|, |\omega_2|, |\omega_3|, ..., |\omega_{n_-}|\}$ for $\omega_i < 0$.

Finally, we discriminate between the different models using the Akaike weights system [*Burnham and Anderson*, 2002], which is a statistical method for comparing the likelihood of two or more model fits to a data set. The Akaike Information Criterion (AIC) [*Akaike*, 1973] for a model i ($i = 1, 2, 3$ here) is

$$\mathrm{AIC}_i = -2 \log \left[\mathcal{L}_i \left(\hat{\boldsymbol{\theta}}_{\boldsymbol{i}} | \boldsymbol{\omega} \right) \right] + 2K_i \tag{4}$$

where $\mathcal{L}$ is the likelihood function, where $\hat{\boldsymbol{\theta}}_{\mathbf{1}} = \hat{\lambda}$, $\hat{\boldsymbol{\theta}}_{\mathbf{2}} = (\hat{c}, \hat{\chi})$, and $\hat{\boldsymbol{\theta}}_{\mathbf{3}} = (\hat{q}, \hat{\kappa})$ for our three model distributions, and where K_i is the number of parameters being estimated for model i. The most likely model is the one with the minimum AIC, termed $\mathrm{AIC}_{\min}$. The Akaike weights are the relative likelihoods of each model, given by

$$W_i = \frac{e^{-\Delta_i/2}}{\sum_{j=1}^{3} e^{-\Delta_j/2}} \tag{5}$$

where $\Delta_i = \mathrm{AIC}_i - \mathrm{AIC}_{\min}$. Hence, the maximum weight is given to the model with minimum AIC, for which $\Delta_i = 0$. The weights are normalised so that they sum to 1. The weight W_i is considered to be the weight of evidence in favour of model i being the best model for the given data, out of the models considered.

3. Results

Figure 1a presents the PDF of all measured vorticity values (grey-shaded histogram), on log-linear axes, with a vorticity bin size of 0.5 mHz. The PDF is distinctly not Gaussian, which would be an inverse parabola on a log-linear plot. Instead it is heavy tailed, i.e., fatter than exponential, which would be a straight line. The maximum likelihood exponential PDFs, for positive and negative vorticity separately, are shown by the green lines and can be seen to underestimate the tails of the distribution. Weibull PDFs (blue

curves) appear to provide better fits than the exponential distribution but still do not accurately describe the tails of the distribution. Q-exponentials (red lines) appear to provide the best fit to the data of the three chosen functions. Indeed the corresponding Akaike weights of the three models are $W_i = \{\sim 0, \sim 0, \sim 1\}$ for both the positive and negative vorticity distributions, confirming that the q-exponential (model 3) is the most likely model out of the three models that we have selected. The high degree of certainty in the model selection (giving weights of effectively 1 and 0) is due to the large number of data points involved in the MLE analysis. That is, the more data we have, the easier it is to clearly distinguish between different models.

Even so, it is evident that the q-exponential may still not fully describe the vorticity distribution. One reason may be that it combines observations from all available AACGM latitudes and MLTs, whereas there are significant spatial variations in average vorticity with latitude and MLT [*Chisham et al.*, 2009] and hence there must similarly be spatial variations in the vorticity PDF. To investigate this we present, in figures 1b-1d, three vorticity PDFs (grey shaded histograms) compiled using vorticity data from three different spatial regions: (b) 67°-70° AACGM latitude, 1800-2100 MLT (typical of the auroral zone), (c) 72°-75° AACGM latitude, 1200-1500 MLT (typical of the cusp), (d) 75°-78° AACGM latitude, 0600-0900 MLT (typical of the polar cap).

As before, we fit our three model distributions to each of the measured vorticity PDFs using maximum likelihood estimates, and then select the most likely of the three models in each case using Akaike weights. In figure 1b, the PDF is more leptokurtic than that shown in figure 1a, but the Akaike weights analysis again suggests that the q-exponential

(red curve) is the best fit to the PDF with $W_{+i} = W_{-i} = \{\sim 0, \sim 0, \sim 1\}$. For figure 1c, the three model curves for positive vorticity are extremely similar, and all fit the PDF well, suggesting that the PDF is close to being exponential. The Akaike weights suggest that all three models are viable, with $W_{+i} = \{0.14, 0.11, 0.75\}$, but with the q-exponential (model 3) being the most likely. For the negative vorticity curve in figure 1c the Akaike weights ($W_{-i} = \{\sim 0, \sim 1, \sim 0\}$) support the Weibull fit (blue curve), highlighting that the q-exponential curve does not always provide the most likely fit to the vorticity PDF at all locations. The vorticity PDF presented in figure 1d is highly asymmetric, with the positive (negative) vorticity PDF being more (less) leptokurtic than the exponential curve. The Akaike weights analysis results in $W_{+i} = \{\sim 0, \sim 0, \sim 1\}$ and $W_{-i} = \{\sim 0, \sim 1, \sim 0\}$ implying that the q-exponential fits best to the positive vorticity PDF and the Weibull fits best to the negative vorticity PDF.

In summary, these three PDFs highlight the following: (1) The PDFs in different spatial regions have different forms, with some being more leptokurtic than others. (2) Some of the PDFs are highly asymmetric around zero vorticity (justifying our decision to treat the positive and negative vorticity distributions separately). (3) The overall vorticity PDF presented in figure 1a is a conglomeration of a number of different vorticity PDFs that characterise different regions.

Given this, we have investigated how the model varies across the whole polar ionosphere by dividing the northern polar ionosphere into regions of 1-hr of MLT by 2° of AACGM latitude and then performing the MLE and Akaike weights analysis on the vorticity data in each region. In figure 2 we present maps which illustrate the spatial variation of the

Akaike weights for the three different models for both positive and negative vorticity. The darkest brown indicates regions where the weight is ∼1, and the lightest brown indicates regions where the weight is ∼0. For both polarities of vorticity the exponential distribution is characterised by low Akaike weights across the majority of the polar ionosphere. The q-exponential distribution is the most likely model for the PDF across most of the polar ionosphere, except for a region in the afternoon sector ionosphere extending from ∼69°-79°AACGM latitude, and from ∼1000-1700 MLT, for positive vorticity, and a similar region extending from ∼0400-1400 MLT for negative vorticity. In both these regions the Weibull is generally the most likely model. (There are other, much smaller, regions where the q-exponential is not the most likely model but here we focus on the gross features of the maps).

4. Discussion

We have found that the PDF of ionospheric vorticity is generally of q-exponential or Weibull form, depending on location. In particular, the Weibull regions match closely to the dayside part of the region 1 field-aligned current (FAC) region where the average vorticity has the largest values for each polarity [*Chisham et al.*, 2009]. This suggests that ionospheric vorticity is generated by different physical mechanisms in different regions of the magnetosphere. A complete physical theory is beyond the scope of this paper but here we outline an explanation.

Consider a magnetohydrodynamic fluid of density ρ and velocity $\mathbf{v} = \mathbf{E} \times \mathbf{B}/\mathbf{B^2}$ in an electric field $\mathbf{E}$ and magnetic field $\mathbf{B}$. Then combining the single fluid momentum

equation and the generalised Ohm's law and taking the curl, we find that the vorticity $\omega = \nabla \times \mathbf{v}$ is given by the classic baroclinic vorticity equation

$$\frac{\partial \omega}{\partial t} = \nabla \times (\mathbf{v} \times \omega) + \frac{\nabla \rho \times \nabla \mathbf{p}}{\rho^{\mathbf{2}}} \tag{6}$$

where p is the ion pressure.

Now separating velocity $\mathbf{v}$ into a deterministic part and a stochastic part corresponding to unresolved or otherwise unrepresented processes, we find that the vorticity equation can be written in the form of a general Langevin equation

$$d\omega_t = f(\omega) + g(\omega)\xi(t) + \eta(t) + h \tag{7}$$

where ξ and η are independent Gaussian white noises representing the unrepresented processes, and h is a constant. Here the multiplicative noise term $(g(\omega)\xi(t))$ corresponds to the convective (first) term on the right-hand side of the vorticity equation (6) and the additive noise term $(\eta(t))$ corresponds to the baroclinic (second) term.

In the general case where both terms are important, the q-exponential is a stationary solution of the corresponding Fokker-Planck equation, assuming $g(\omega)$ to be of power law form and f to be constant [e.g., *Anteneodo and Tsallis*, 2003]. An example of this would be in the region 2 current region where the plasma pressure gradient is expected to be significant [e.g., *Southwood*, 1977]. However in the absence of the baroclinic additive noise term, a Weibull solution of the stationary Fokker-Planck equation is instead possible, assuming g and f to have the same power law dependency. This could be expected in the region 1 current region where the plasma pressure is less important. Thus the general

morphology of ionospheric vorticity is explained by the relative importance of convective and baroclinic effects. A more detailed derivation and analysis will be presented elsewhere.

It is interesting to note that similar arguments might apply to FACs, which are closely associated with vorticity [e.g., *Southwood and Kivelson*, 1991]. Thus we might expect their distributions to be of similar heavy-tailed form. Indeed, a long-tailed distribution of 'intense kilometre-scale' FAC densities has been reported [*Rother et al.*, 2007] but this was of peak currents in an 'event', not of all FAC measurements, and no attempt was made to model the distribution or even to assess whether it was leptokurtic or heavy-tailed. Nevertheless, extreme FAC densities of order 1 mA m^{-2} were measured, which greatly exceeded typical large-scale average current densities of order 1μA m^{-2}. This motivates closer examination and identification of the FAC distribution and its variation with measurement scale, which we will do in a future study. In general, having a model for the PDF allows us to estimate the likelihood of extreme events, even beyond those already observed. This may have application in assessing natural hazards to satellites, such as single event upsets from particle acceleration caused by extreme FACs.

5. Summary

Distributions of ionospheric vorticity, as measured by the SuperDARN radars, are distinctly non-Gaussian with typically heavy tails. The PDFs in different regions of the ionosphere are well approximated by either q-exponential or Weibull probability density functions. Weibull PDFs appear to fit best in the dayside region 1 field-aligned current region whereas q-exponential PDFs appear to fit best elsewhere. These distributions can be explained by the relative importance of different physical mechanisms for generating

vorticity in the different regions. Such knowledge will allow us to estimate the probability of observing extreme values of vorticity, and likely also of FAC, and also to assess associated natural hazards.

Acknowledgments. We are extremely grateful to G.J. Sofko and W.A. Bristow, the PIs of the Prince George and Kodiak SuperDARN radars, respectively. We would like to thank G.A. Abel for help with the vorticity determination method, and N.W. Watkins for discussions about potential model PDFs. The authors are supported by the UK Natural Environment Research Council through the Complexity workpackage of the BAS Environmental Change and Evolution programme.

References

Akaike, H. (1973), Information theory as an extension of the maximum likelihood principle, pp.267-281, in B. N. Petrov and F. Csaki (eds.), Second international symposium on information theory, Akademiai Kiado, Budapest.

Anteneodo, C., and C. Tsallis (2003), Multiplicative noise: A mechanism leading to nonextensive statistical mechanics, *J. Math. Phys.*, *44*, 5194-5203

Burnham, K. P., and D. R. Anderson (2002), *Model selection and multimodel inference: A practical information-theoretic approach*, 2nd edn, Springer, New York.

Chisham, G., M. P. Freeman, G. A. Abel, W. A. Bristow, A. Marchaudon, J. M. Ruohoniemi, and G. J. Sofko (2009), Spatial distribution of average vorticity in the high-latitude ionosphere and its variation with interplanetary magnetic field direction and season, *J. Geophys. Res.*, *114*, A09301, doi:10.1029/2009JA014263.

199 Chisham, G., et al. (2007), A decade of the Super Dual Auroral Radar Network (Super-
200 DARN): scientific achievements, new techniques and future directions, *Surv. Geophys.*,
201 *28*, 33-109.

202 Edwards, A. M., et al. (2007), Revisiting Lévy flight search patterns of wandering alba-
203 trosses, bumblebees and deer, *Nature*, *449*, 1044-1048.

204 Golovchanskaya, I. V. (2008), Assessment of Joule heating for the observed
205 distributions of high-latitude electric fields, *Geophys. Res. Lett.*, *35*, L16102,
206 doi:10.1029/2008GL034413.

207 Greenwald, R. A., et al. (1995), DARN/SuperDARN: a global view of the dynamics of
208 high-latitude convection, *Space Sci. Rev.*, *71*, 761-796.

209 Hnat, B., S. C. Chapman, and G. Rowlands (2005), Scaling and a Fokker-Planck model
210 for fluctuations in geomagnetic indices and comparison with solar wind ϵ as seen by
211 Wind and ACE, *J. Geophys. Res.*, *110*, A08206, doi:10.1029/2004JA010824.

212 Mandelbrot, B., and R. L. Hudson (2004), The (mis)behaviour of markets : a fractal view
213 of risk, ruin and reward, London : Profile, ISBN 1861977654.

214 Qiao, H. Z., and C. P. Tsokos (1994), Parameter estimation of the Weibull probability
215 distribution, *Mathematics and Computers in Simulation*, *37*, 47-55.

216 Rother, M., K. Schlegel, and H. Lühr (2007), CHAMP observation of intense kilometer-
217 scale field-aligned currents, evidence for an ionospheric Alfvén resonator, *Ann. Geophys.*,
218 *25*, 1603-1615.

219 Shalizi, C. R. (2007), Maximum likelihood estimation for q-exponential (Tsallis) distribu-
220 tions, arXiv:math/0701854v2.

Sornette, D. (2003), *Critical Phenomena in Natural Sciences. Chaos, Fractals, Selforganization and Disorder: Concepts and Tools*, pp. 185-186, 2nd edn, Springer-Verlag, Berlin, Heidelberg, New York.

Southwood, D. J., and M. Kivelson (1991), An Approximate Description of Field-Aligned Currents in a Planetary Magnetic Field, *J. Geophys. Res.*, *96*, 67-75.

Southwood, D. J. (1977), The role of hot plasma in magnetospheric convection, *J. Geophys. Res.*, *82*, 55125520

Figure 1. Probability density functions of ionospheric vorticity for (a) all vorticity measurements, (b) vorticity measurements between 67°-70°AACGM latitude and 1800 and 2100 MLT, (c) vorticity measurements between 72°-75°AACGM latitude and 1200 and 1500 MLT, (d) vorticity measurements between 75°-78°AACGM latitude and 0600 and 0900 MLT. The green, blue, and red lines represent MLE exponential, weibull, and q-exponential fits to the vorticity data, respectively.

Figure 2. Spatial variation across the polar ionosphere of Akaike weights for q-exponential, weibull, and exponential distributions, and for positive and negative vorticity measurements.

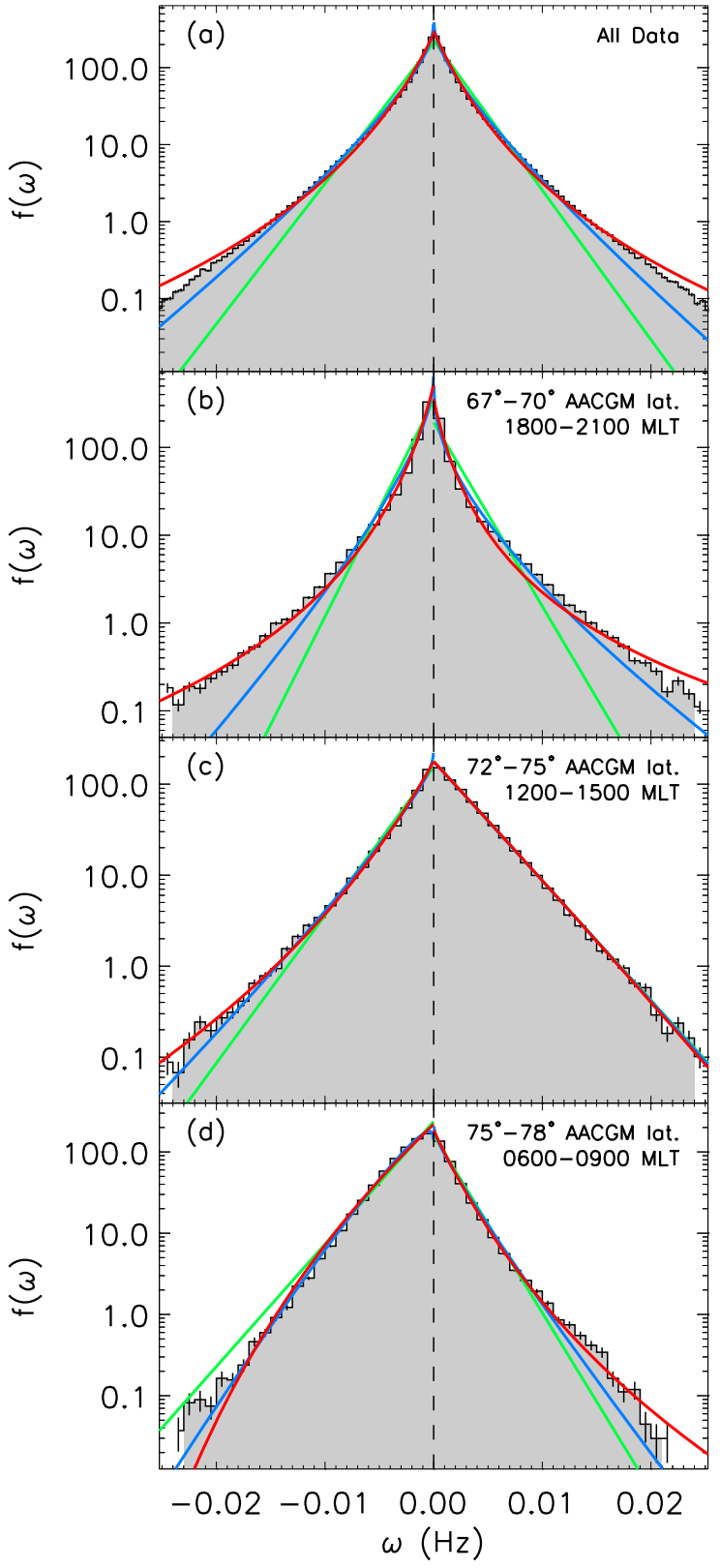
(a)
All Data
(b)
67°–70° AACGM lat.
1800–2100 MLT
(c)
72°–75° AACGM lat.
1200–1500 MLT
(d)
75°–78° AACGM lat.
0600–0900 MLT
f(ω)
100.0
10.0
1.0
0.1
−0.02
−0.01
0.00
0.01
0.02
ω (Hz)

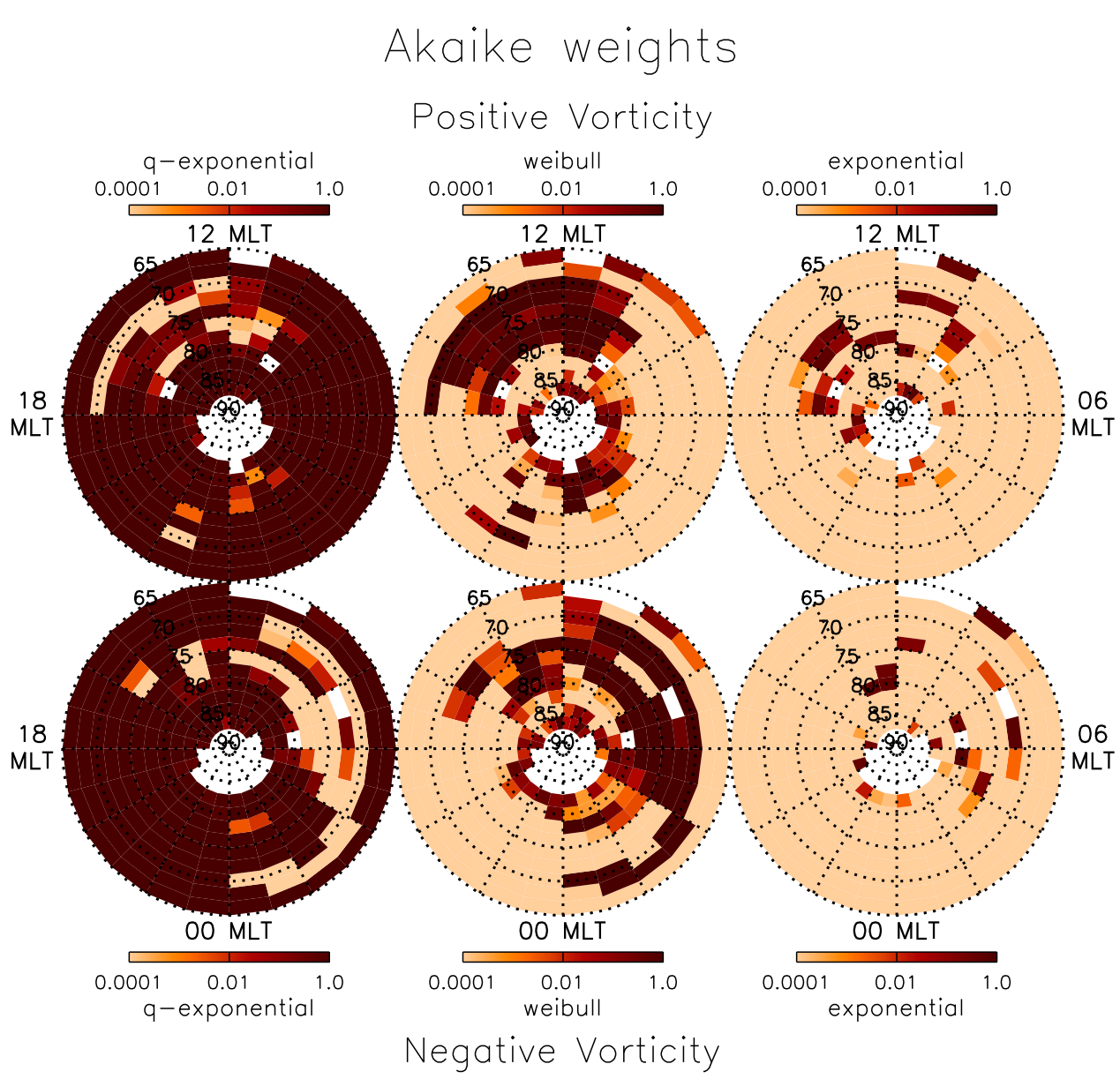
Akaike weights
Positive Vorticity
q−exponential
0.0001
0.01
1.0
weibull
0.0001
0.01
1.0
exponential
0.0001
0.01
1.0
12 MLT
18 MLT
06 MLT
00 MLT
65
70
75
80
85
90
Negative Vorticity